Supplement material for the paper

Long-term aerosol optical hygroscopicity study at the ACTRIS SIRTA observatory: synergy between ceilometer and in-situ measurements

Andrés Esteban Bedoya-Velásquez [1,2,3], Gloria Titos [1,2,4], Juan Antonio Bravo-Aranda [1,2], Martial Haeffelin[5], Olivier Favez[6], Jean-Eudes Petit[7], Juan Andrés Casquero-Vera[1,2], Francisco José Olmo-Reyes[1,2], Elena Montilla-Rosero[8], Carlos D. Hoyos[9], Lucas Alados-Arboledas [1,2] and Juan Luis Guerrero- Rascado [1,2].

1 Effect of beta-attenuated water vapor correction on calculated $f_{\beta}(RH)$ and γ parameter

The β^{att} signal presents a dependency on water vapor absorption as shown in Sec. 4.2 (Eq. 7), associated with the wavelength emission. This dependency may cause direct effects over calculations retrieved by using β^{att}. Here, we present the correction applied to β^{att} and the effects on $f_{\beta}(RH)$ and γ calculations. Figure S1 (left-panels) represents the temporal-evolution of β^{att}, beta attenuated water vapour corrected (β_{wv}^{att}) signals over 3 h time-window, together with the temporal-evolution of q. . Figure S1 (right-panels) shows the biases for beta ($bias_{\beta}$) and Δ_q obtained.

The quantifications are performed by means of the $bias_{\beta}$ ($\beta^{att} - \beta_{wv}^{att}$) and Δ_q $\left(q(t) - q\ (t_d)\right)$ calculations. Fig. S1ac presents two cases (case 1 and case 2) with low absolute-differences in q, which produces slight changes in β_{wv}^{att} signal respect to β^{att}. On the other hand, Fig. S1eg (case 3 and case 4) show that high absolute-differences in q are linked to high changes on β_{wv}^{att}. The right side of the panel (Fig. 1Sbd, case 1 and case 2), presents the bias quantification, showing that low $bias_{\beta}$ are associated with low Δ_q and, on the contrary, Fig. 1Sfh (case 3 and case 4), show that increases in Δ_q makes that $bias_{\beta}$ becomes higher. This analysis leads us to conclude that no-water vapor correction will produce an overestimation of the total β signal, being $\Delta_q$the parameter that rules the β correction. From now, we will use β instead of β^{att} for simplicity.

To see the effect of β_{wv}^{att} on $f_{\beta}(RH)$, we applied the Hännel parameterization (Eq. 6, Sec. 4.1 of the manuscript) to the same 4 cases studied above. Figure S2 presents the $f_{\beta}(RH)$ and the enhancement factor water vapour corrected, $f_{\beta_{wv}^{att}}(RH)$. The results reinforce those obtained above (Fig S1), where low/high changes in Δ_q are linked with low/high $bias_{\beta}$ and, on this way, this would affect $f_{\beta}(RH)$ calculation. Additionally, the water vapour correction tends to decrease γ (β_{wv}^{att} is lower than β). Therefore, cases with lower $bias_{\beta}$ and Δ_q (case 1 and case 2), exhibits lower $bias_{\gamma}$ (0.02 and 0.05, respectively), meanwhile on case 3 and case 4 instead $bias_{\beta}$ increase, the $bias_{\gamma}$ becomes higher (0.11 and 0.09, respectively).

Once we applied the phase 2 of the methodology (Sec. 5), we obtain 94 hygroscopic potential cases for 3h time-window (Fig. S3a), 9 cases for 4h time-window (Fig. S3a) and 4 cases for 5h time-window (Fig. S3a), resulting in a total of 107 cases. To establish a bias error for this hygroscopic study, we have calculated the median of the $bias_{\beta}$ and Δ_q, highlighting two main aspects: (i) The median $bias_{\beta}$ follows the median Δ_q variability, remarking their dependency. This fact is well seen from the scatter plot (Fig. 3Sb), where these variables show a positive correlation, however the correlation coefficient is not too high (R^2= 0.61), mainly because the data dispersion increases for $bias_{\beta}$ > 1.5 10^{-7} $m^{-1}\cdot sr^{-1}$ and Δ_q > 3.0 g/m^3; (ii) The mean bias error calculated for β_{wv}^{att} over the 107 potential cases evaluated is lower than $2.5\cdot10^{-7}$ $m^{-1}\cdot sr^{-1}$ and the mean Δ_q is lower than 5.5 g/m^3.

Fig. S4 quantifies the effect of the β_{wv}^{att} over $f_{\beta}(RH)$ and γ hygroscopic properties, by means of the median $bias_{f_{\beta}(RH)}$ ($f_{\beta}(RH)$ - $f_{\beta_{wv}^{att}}(RH)$) and the bias $_{\gamma}$ ($\gamma_{\beta^{att}} - \gamma_{\beta_{wv}^{att}}$). Figure S4 reveals the no-correlation between $bias_{\beta}$ and $bias_{f_{\beta}(RH)}$. However, combining the results from Fig. S3 and Fig. S4, it is possible to establish that $bias_{\beta}$ > 1 $m^{-1}\cdot sr^{-1}$ would cause an increment of $bias_{f_{\beta}(RH)}$ above 0.2, increasing the error on $f_{\beta}(RH)$. Finally, it was obtained that $bias_{f_{\beta}(RH)}$ and bias $_{\gamma}$ for the whole study were lower than 0.3.

2 Results

2.1 Methodology applied to eight aerosol hygroscopic growth cases

The 8 hygroscopic growth cases reported in this study (Table 1, Sec. 6.2) were found at daytime in the early morning, with RH_{ref} around 50 % and the maximum RH reached was up to 90% over 3h time-window. For cases 1, 2, 4, 5, 6 and 7 the perceptual composition was dominated by OA with values up to 50 %, except on case 7 where OA decreased up to 38%. The BC concentration was relatively low almost for all cases found (close to 6 %). The concentration of inorganic compounds were dominated by SO_4^{2-} (lower than 21 %) and NH_4^+(lower than 19 %), however NO_3^- reached values of 21% on case 6. The air masses that come mainly from W-NW direction are related to case 1 (Δu=3.6 m/s W), case 2 (Δu=23.0 m/s NW) and case 6 (Δu=4.4 m/s W), with speed variability up to 14.2 %, 20.7 % and 18.5 %, respectively; and the air masses that coming from W-SW direction at low wind direction variability are associated with case 4 (Δu=2.7 m/s W), case 5 (Δu=2.4 m/s SW), and case 7 (Δu=1.7 m/s SW), and wind speed variability about 15.4 m/s, 20.4 m/s and 10.9 m/s, respectively. All these cases fulfilled the threshold established for $\frac{\Delta f_{PM1}(RH)}{\Delta f_{\beta}(RH)} < 0.5$ indicating that increases/decreases in $f_{\beta}(RH)$ are not related with advected aerosol into the atmospheric volume studied. The Hännel parameterization is calculated for both $f_{\beta}(RH)$ and $f_{PM1}(RH)$ (see panel Fig. S4 to S9 b.). The hygroscopicity properties of the 6 cases presented here were evaluated and compared against literature in the Sec. 6.2 of the article.

References

Draxler, R. R. and Rolph, G. D.: HYSPLIT (HYbrid Single-Particle Lagrangian Integrated Trajectory) Model access via NOAA ARL READY, http://ready.arl.noaa.gov/HYSPLIT.php (last access: July 2010), NOAA Air Resources Laboratory, Silver Spring, MD, 2012.

Zhang, L., Sun, J.Y., Shen, X.J., Zhang, Y.M., Che, H.C., Ma, Q.L., Zhang, Y.W., Zhang, X.Y., Ogren, J.A.: Observations of relative humidity effects on aerosol light scattering in the Yangtze River Delta of China. Atmos. Chem. Phys.15, 8439e8454. http://dx.doi.org/10.5194/acpd-15-2853-2015, 2015.

Zieger, P., Fierz-Schmidhauser, R., Poulain, L., Müller, T., Birmili, W., Spindler, G., Wiedensohler, A., Baltensperger, U., Weingartner, E.: Influence of water uptake on the aerosol particle light scattering coefficients of the Central European aerosol. Tellus B 66, 22716. http://dx.doi.org/10.3402/tellusb.v66.22716, 2014.

Figure captions

Figure S1. Time evolution of β^{att}(blue line), β_c^{att}(red line) and q (orange line)[left panels (a,c,e,g $bias_\beta$ (black line) and Δ_q (green line) [right panel (b,d,f,h)].

Figure S2. Experimental data points (blue/red dots) and Hännel parameterization (blue/red lines). Case 1 and Case 2 show the effect of the lower bias_β and Δ_q differences over $f_{\beta_{wv}^{att}}(RH)$ and $f_\beta(RH)$. Case 3 and Case 4 present the effect of the higher bias_β and Δ_q differences over $f_{\beta_{wv}^{att}}(RH)$ and $f_\beta(RH)$.

Figure S3. Median of bias_β and Δ_q for all potential cases of hygroscopic growth found from 2012 to 2016 at the ACTRS SIRTA observatory: (a median of bias_β and Δ_q to 3h time-window analysis (green bars), 4h time-window analysis (orange bars) and 5h time-window analysis (blue bars); (b) scatter plot correlating median of bias_β and Δ_q for whole time-windows.

Figure S4. $\text{bias}_{f_\beta(RH)}$ and $bias_\gamma$ for all potential cases of hygroscopic growth found from 2012 to 2016 at the ACTRIS SIRTA observatory. $\text{bias}_{f_\beta(RH)}$ and bias_γ for 3h time-window analysis (green bars), 4h time-window analysis (orange bars) and 5h time-window analysis (blue bars).

Figure S5. Criterion for data selection: case 1 on 29 July 2012 from 06:30 to 09:30 UTC.

Figure S6. Criterion for data selection: case 2 on 02 September 2012 from 10:30 to 13:30 UTC.

Figure S7. Criterion for data selection: case 4 on 28 July 2014 from 09:10 to 12:10 UTC.

Figure S8. Criterion for data selection: case 5 on 17 August 2014 from 06:40 to 09:40 UTC.

Figure S9. Criterion for data selection: case 6 on 21 May 2015 from 06:15 to 09:15 UTC.

Figure S10. Criterion for data selection: case 7 on 15 April 2016 from 07:05 to 10:05 UTC.

Figure S1:

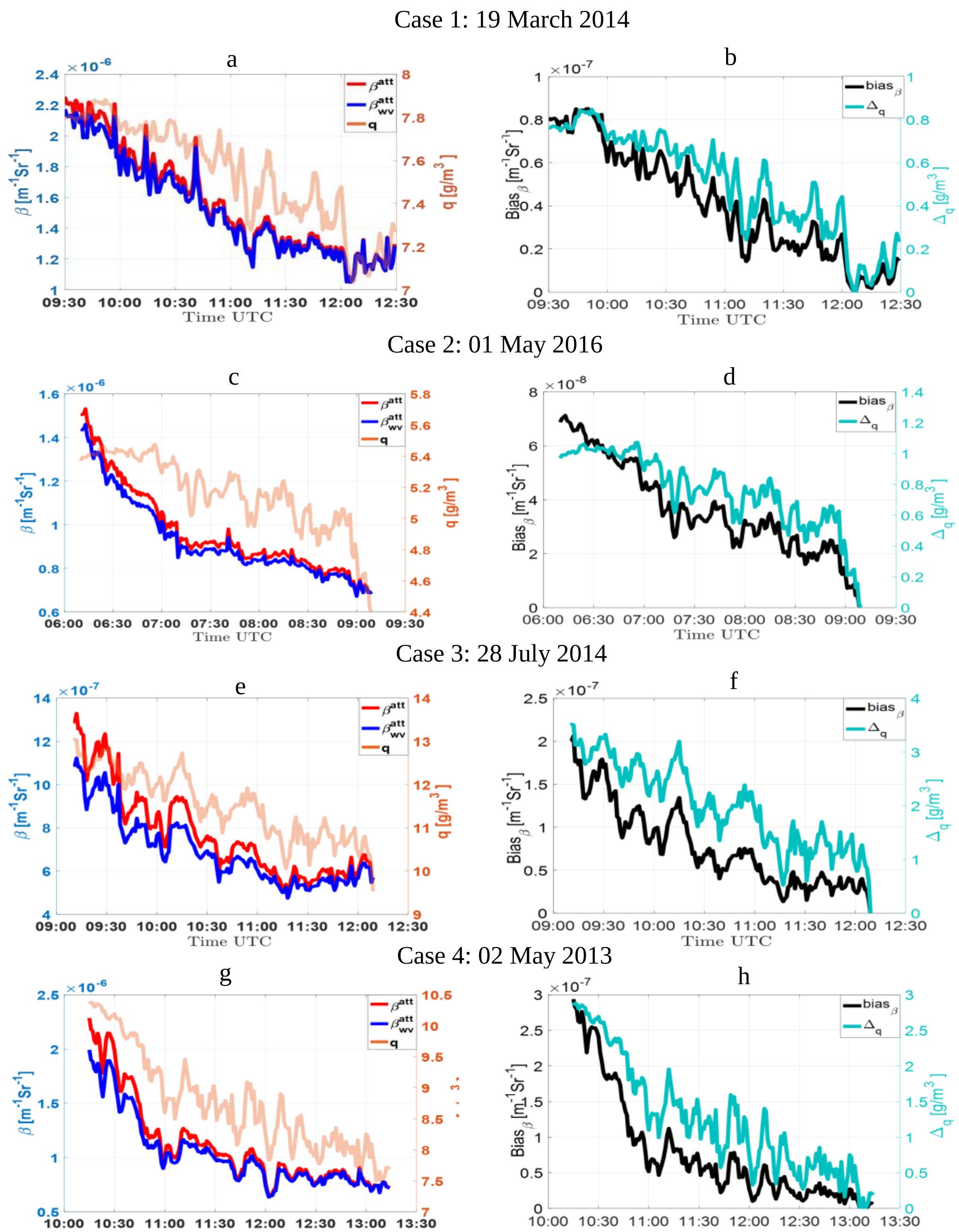

Figure S2:

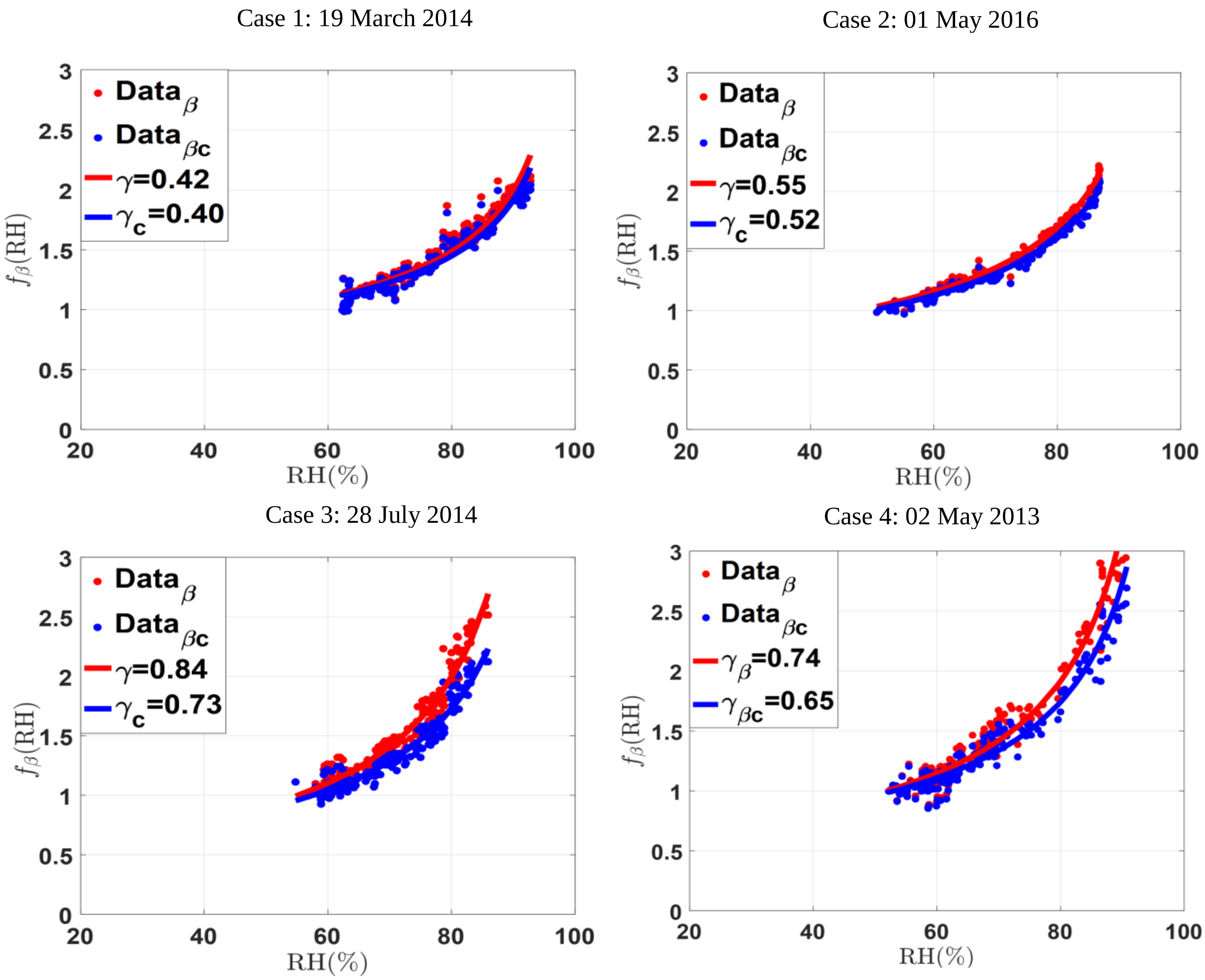
Case 1: 19 March 2014
$Data_{\beta}$
$Data_{\beta c}$
γ=0.42
γ_c=0.40
f_{β}(RH)
RH(%)
Case 2: 01 May 2016
$Data_{\beta}$
$Data_{\beta c}$
γ=0.55
γ_c=0.52
f_{β}(RH)
RH(%)
Case 3: 28 July 2014
$Data_{\beta}$
$Data_{\beta c}$
γ=0.84
γ_c=0.73
f_{β}(RH)
RH(%)
Case 4: 02 May 2013
$Data_{\beta}$
$Data_{\beta c}$
γ_{β}=0.74
$\gamma_{\beta c}$=0.65
f_{β}(RH)
RH(%)

Figure S3:

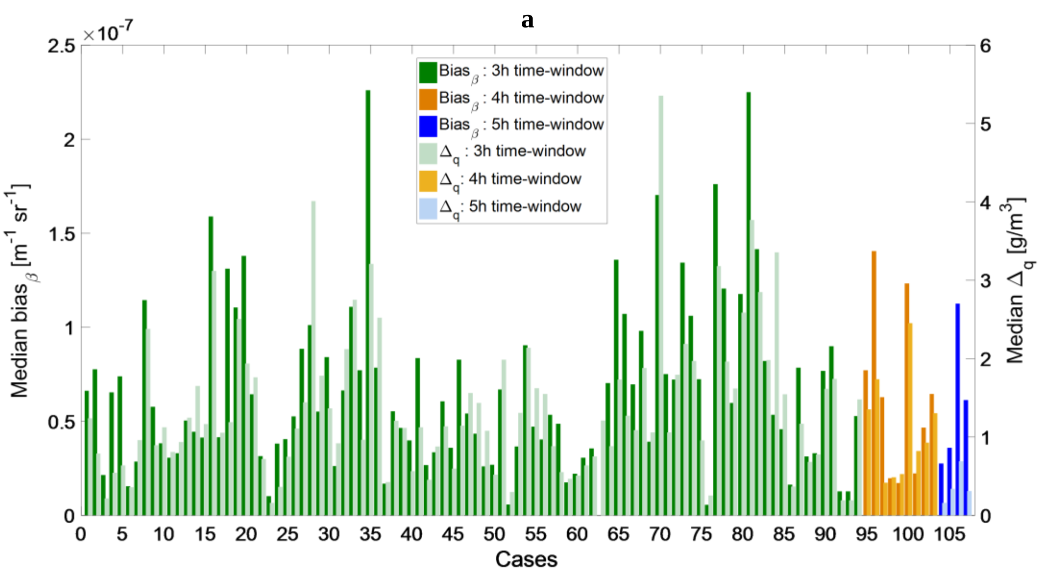
a
×10^-7
Bias_β : 3h time-window
Bias_β : 4h time-window
Bias_β : 5h time-window
Δ_q : 3h time-window
Δ_q: 4h time-window
Δ_q: 5h time-window
Median bias_β [m^-1 sr^-1]
Median Δ_q [g/m^3]
Cases

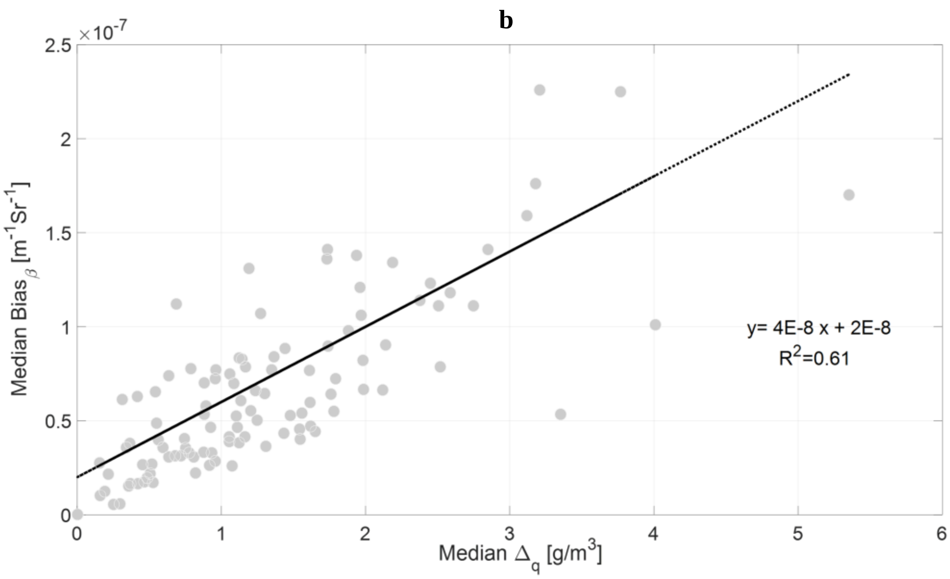
b
×10^-7
y= 4E-8 x + 2E-8
R^2=0.61
Median Bias_β [m^-1Sr^-1]
Median Δ_q [g/m^3]

Figure S4:

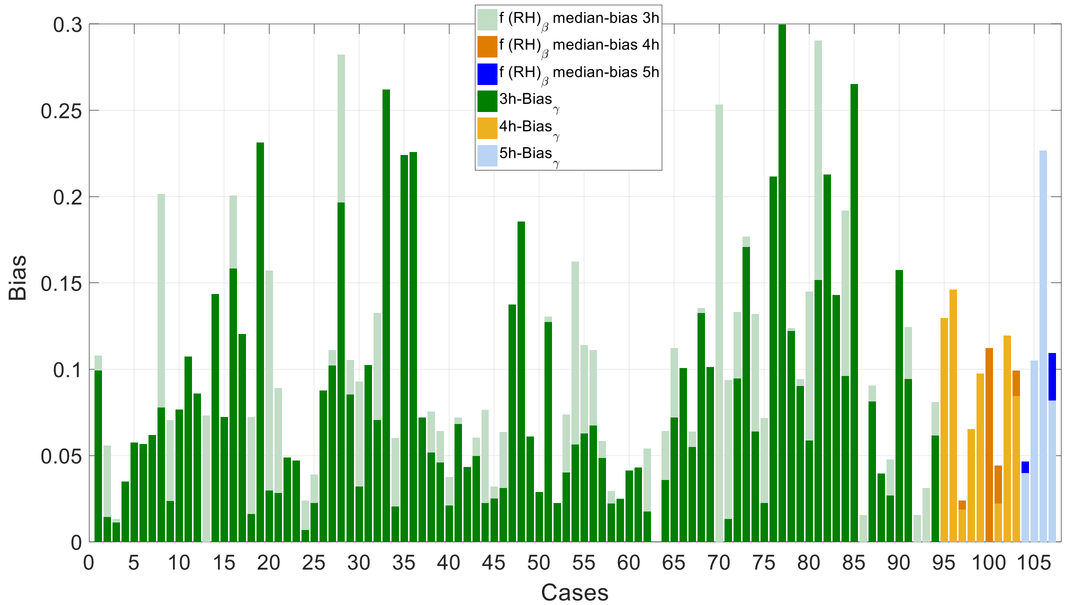

f (RH)β median-bias 3h
f (RH)β median-bias 4h
f (RH)β median-bias 5h
3h-Biasγ
4h-Biasγ
5h-Biasγ
Bias
Cases
0.3
0.25
0.2
0.15
0.1
0.05
0
0 5 10 15 20 25 30 35 40 45 50 55 60 65 70 75 80 85 90 95 100 105

Figure S5:

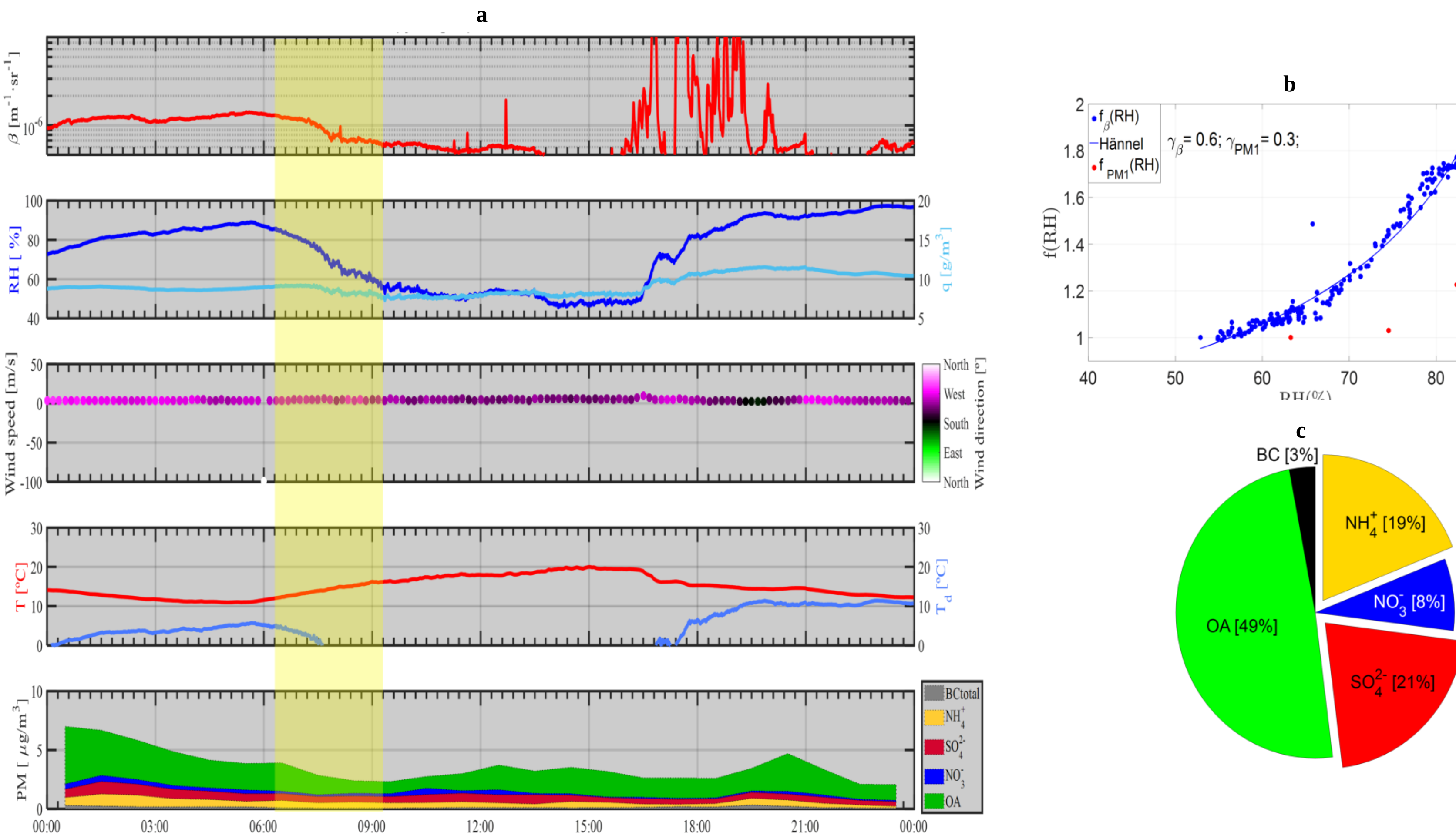
a
β [m⁻¹·sr⁻¹]
10⁻⁶
RH [%]
q [g/m³]
100
80
60
40
20
15
10
5
Wind speed [m/s]
50
0
-50
-100
North
West
South
East
North
Wind direction [°]
T [°C]
T_d [°C]
30
20
10
0
PM [μg/m³]
BCtotal
NH4+
SO4 2-
NO3-
OA
00:00
03:00
06:00
09:00
12:00
15:00
18:00
21:00
00:00
b
f_β(RH)
Hännel
f_PM1(RH)
γ_β = 0.6; γ_PM1 = 0.3;
f(RH)
2
1.8
1.6
1.4
1.2
1
40
50
60
70
80
90
c
BC [3%]
NH4+ [19%]
NO3- [8%]
SO4 2- [21%]
OA [49%]

Figure S6:

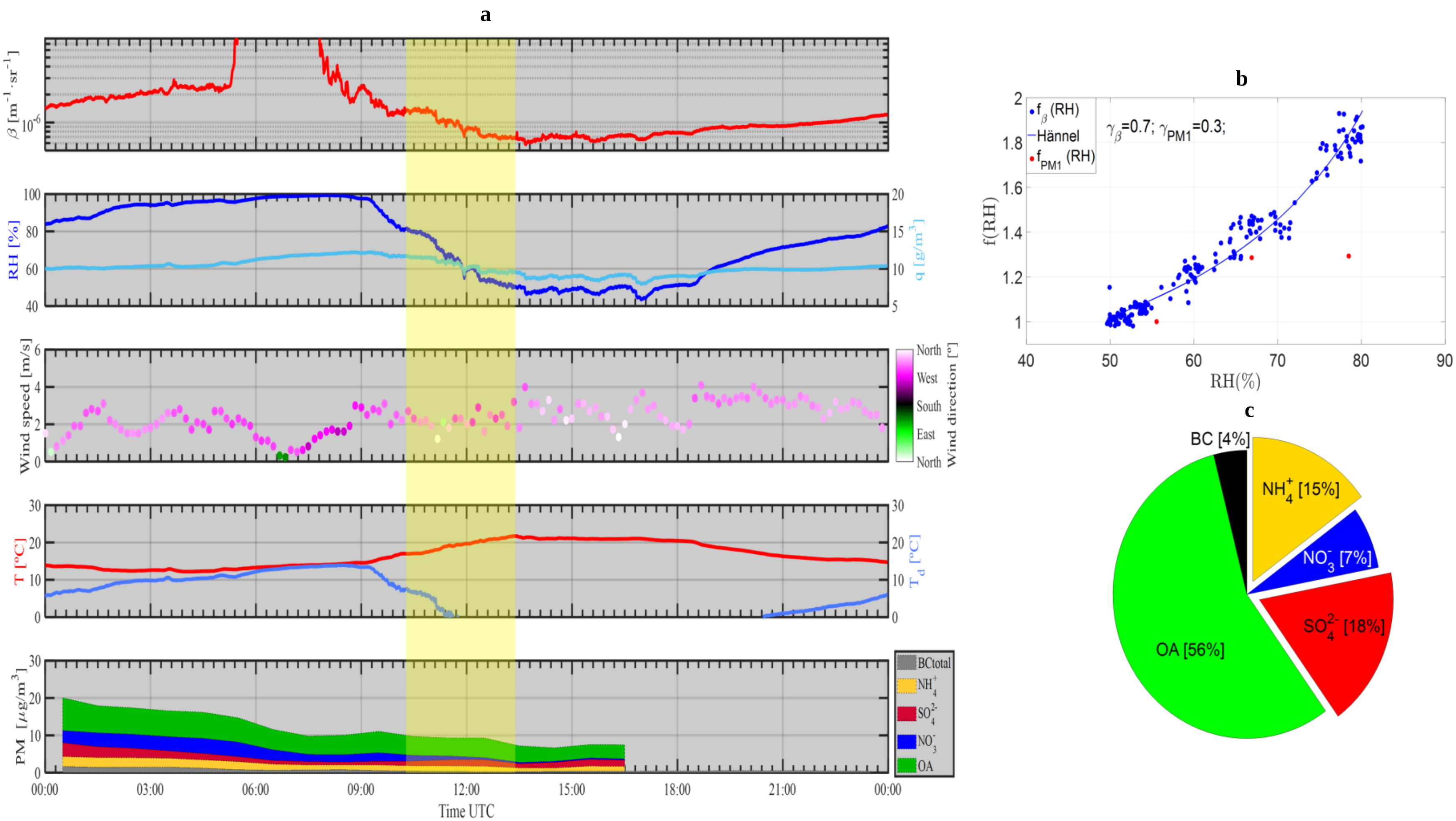

a
β [m⁻¹·sr⁻¹]
10⁻⁶
RH [%]
q [g/m³]
Wind speed [m/s]
Wind direction [°]
North
West
South
East
North
T [°C]
T_d [°C]
PM [μg/m³]
BCtotal
NH4+
SO4 2-
NO3-
OA
00:00
03:00
06:00
09:00
12:00
15:00
18:00
21:00
00:00
Time UTC
b
f_β (RH)
Hännel
f_PM1 (RH)
γ_β=0.7; γ_PM1=0.3;
f(RH)
RH(%)
c
BC [4%]
NH4+ [15%]
NO3- [7%]
SO4 2- [18%]
OA [56%]

Figure S7:

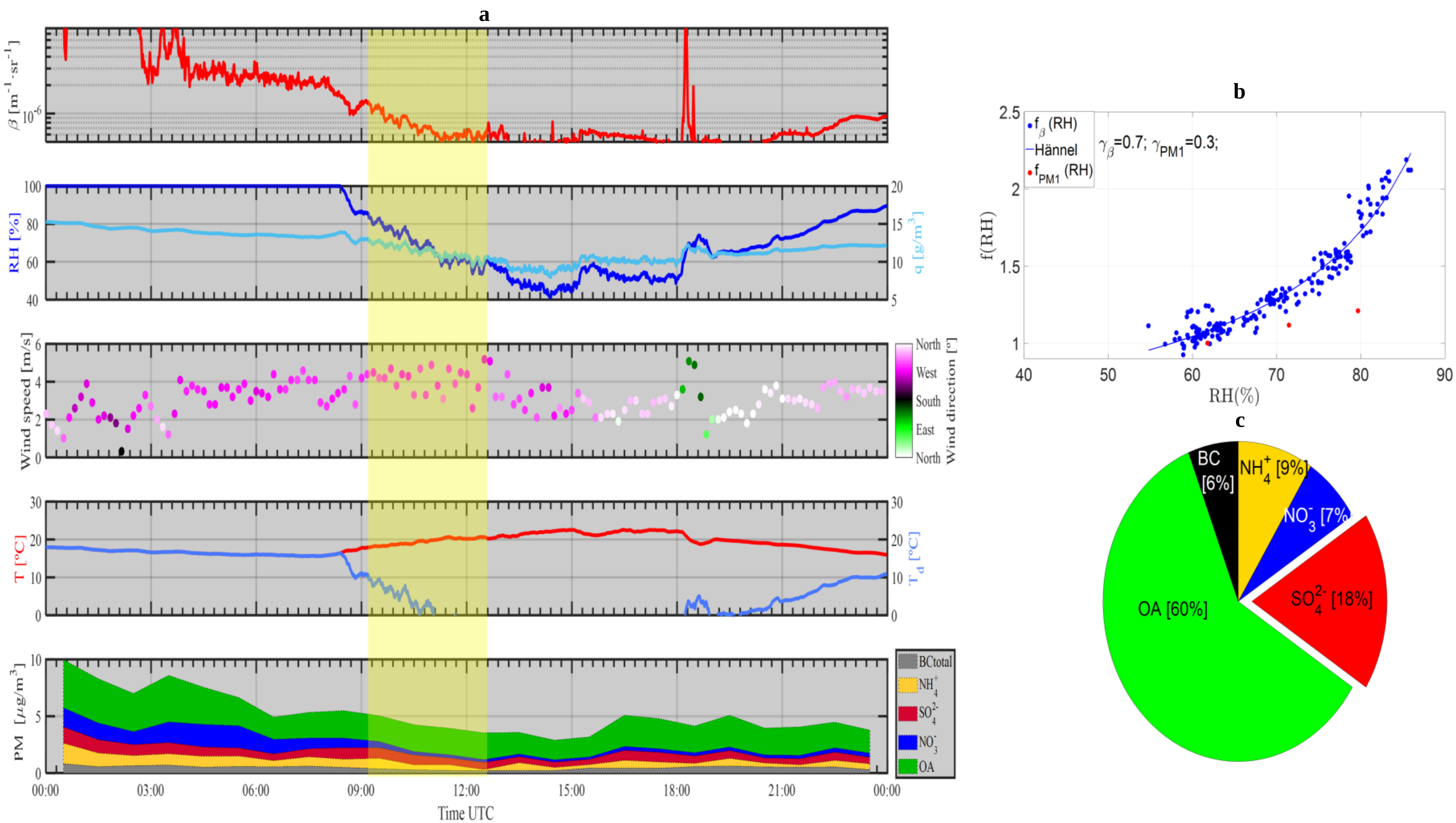
a
β [m⁻¹·sr⁻¹]
10⁻⁶
RH [%]
q [g/m³]
Wind speed [m/s]
Wind direction [°]
North
West
South
East
North
T [°C]
T_d [°C]
PM [μg/m³]
BCtotal
NH4+
SO4 2-
NO3-
OA
00:00
03:00
06:00
09:00
12:00
15:00
18:00
21:00
00:00
Time UTC
b
f_β (RH)
Hännel
f_PM1 (RH)
γ_β=0.7; γ_PM1=0.3;
f(RH)
RH(%)
c
BC [6%]
NH4+ [9%]
NO3- [7%]
SO4 2- [18%]
OA [60%]

Figure S8:

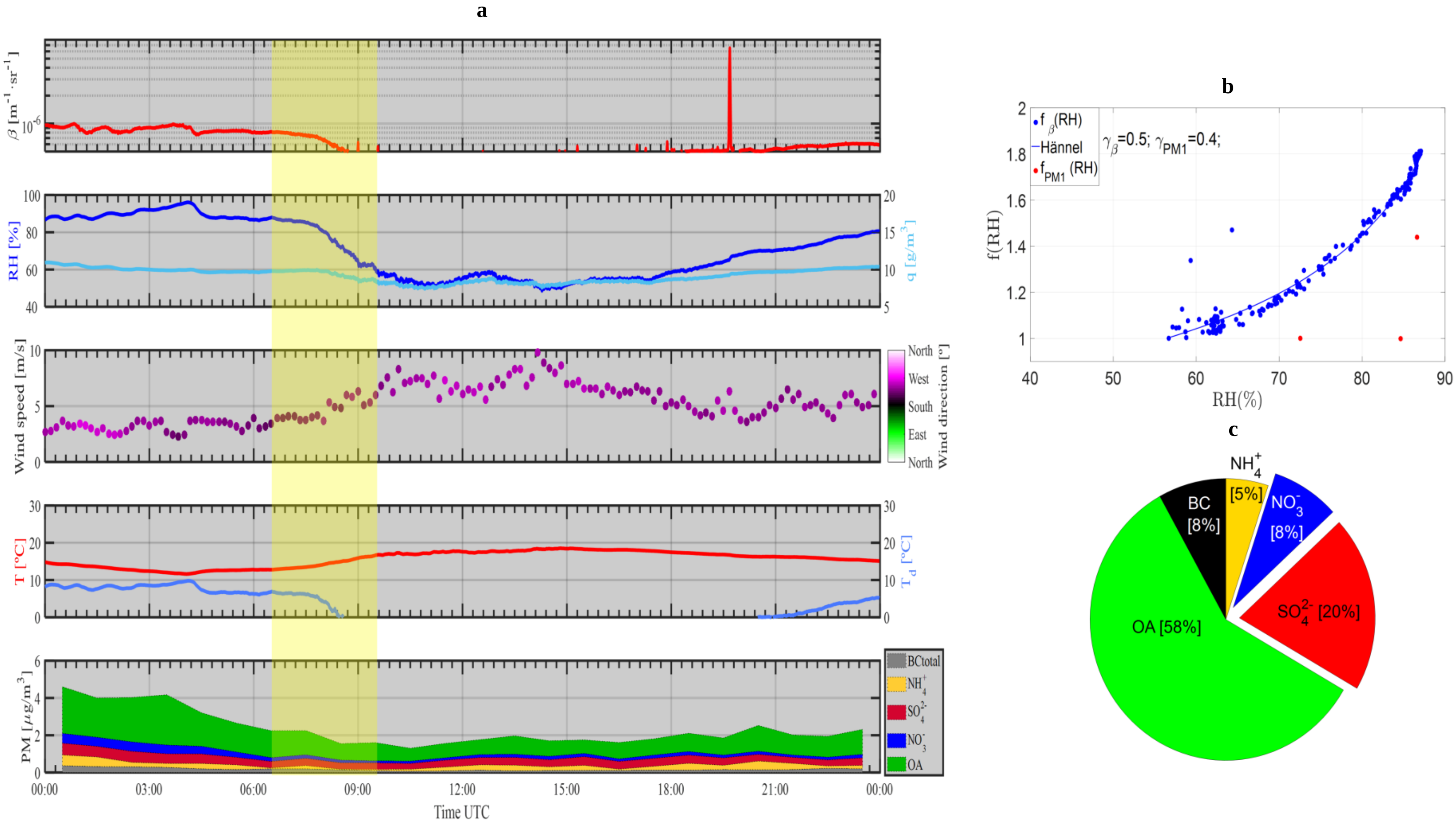
a
β [m⁻¹·sr⁻¹]
10⁻⁶
RH [%]
q [g/m³]
Wind speed [m/s]
Wind direction [°]
North
West
South
East
North
T [°C]
T_d [°C]
PM [μg/m³]
BCtotal
NH₄⁺
SO₄²⁻
NO₃⁻
OA
00:00
03:00
06:00
09:00
12:00
15:00
18:00
21:00
00:00
Time UTC
b
f_β(RH)
Hännel
f_PM1 (RH)
γ_β=0.5; γ_PM1=0.4;
f(RH)
RH(%)
c
NH₄⁺ [5%]
BC [8%]
NO₃⁻ [8%]
SO₄²⁻ [20%]
OA [58%]

Figure S9:

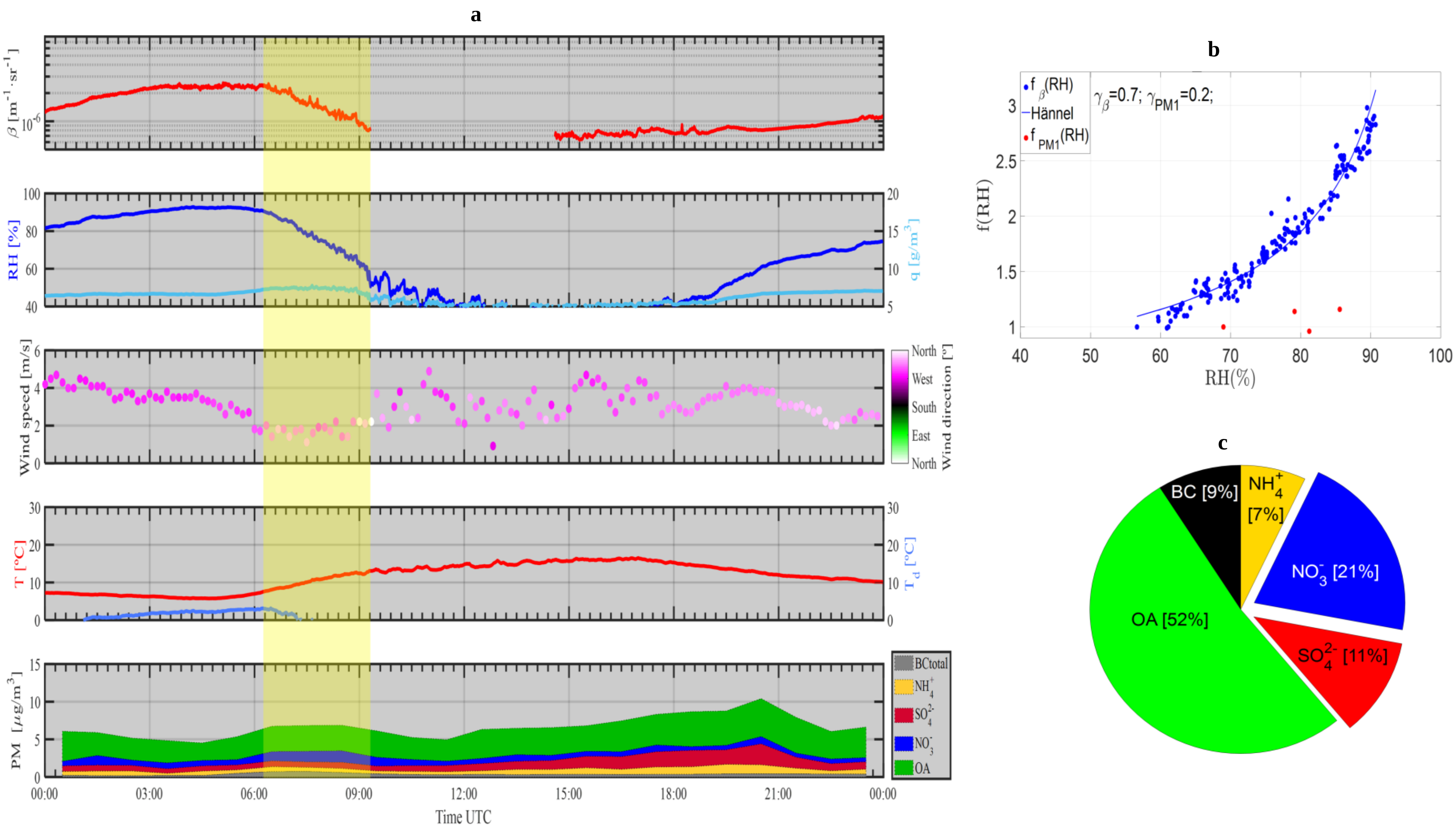
a
b
c
β [m⁻¹·sr⁻¹]
RH [%]
q [g/m³]
Wind speed [m/s]
Wind direction [°]
North
West
South
East
North
T [°C]
T_d [°C]
PM [μg/m³]
BCtotal
NH4+
SO4 2-
NO3-
OA
00:00
03:00
06:00
09:00
12:00
15:00
18:00
21:00
00:00
Time UTC
f_β(RH)
Hännel
f_PM1(RH)
γ_β=0.7; γ_PM1=0.2;
f(RH)
RH(%)
BC [9%]
NH4+ [7%]
NO3- [21%]
SO4 2- [11%]
OA [52%]

Figure S10

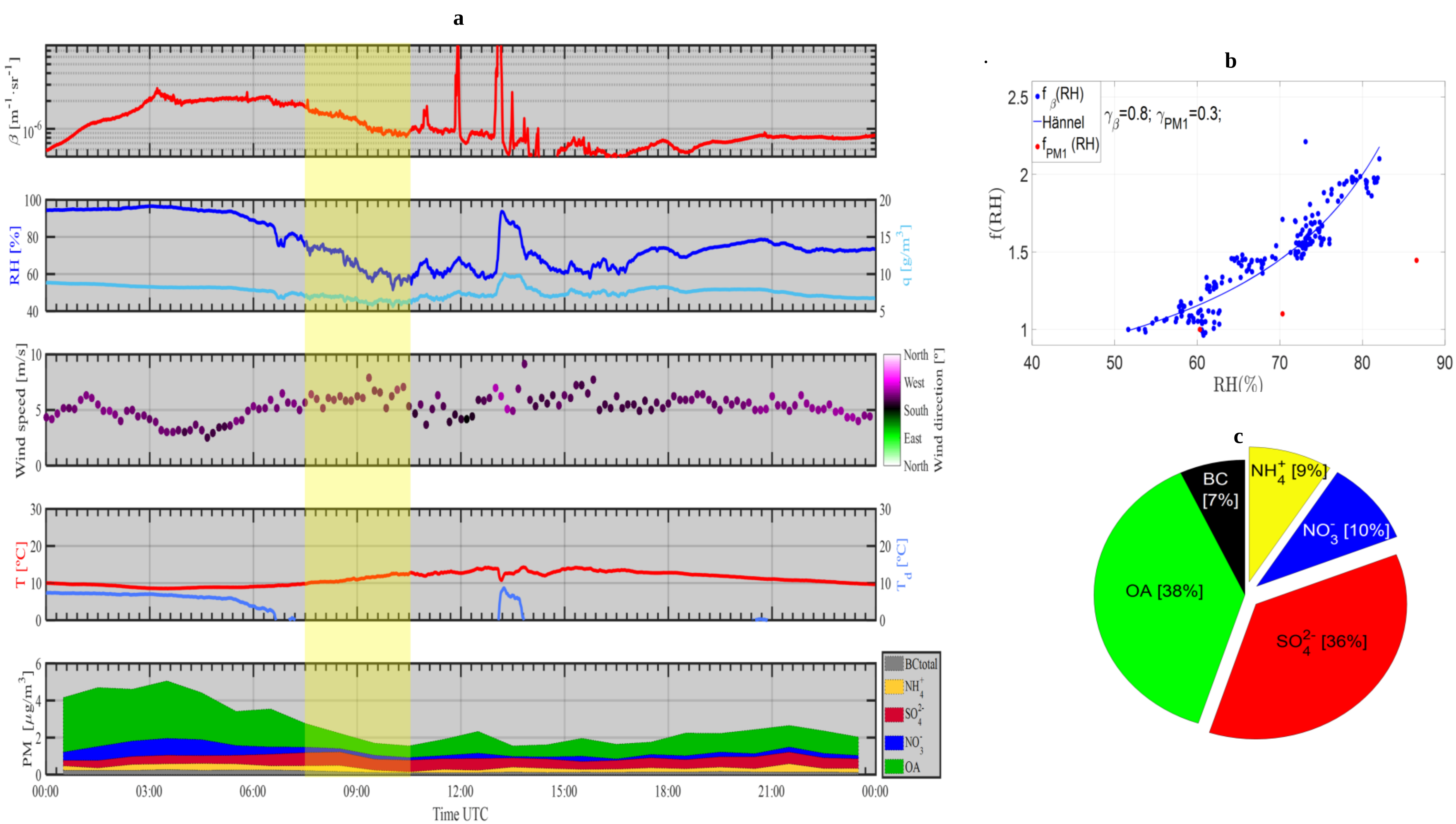
a
β [m⁻¹·sr⁻¹]
10⁻⁶
RH [%]
q [g/m³]
Wind speed [m/s]
Wind direction [°]
North
West
South
East
North
T [°C]
T_d [°C]
PM [µg/m³]
BCtotal
NH₄⁺
SO₄²⁻
NO₃⁻
OA
00:00
03:00
06:00
09:00
12:00
15:00
18:00
21:00
00:00
Time UTC
b
f_β(RH)
Hännel
f_PM1(RH)
γ_β=0.8; γ_PM1=0.3;
f(RH)
RH(%)
c
BC [7%]
NH₄⁺ [9%]
NO₃⁻ [10%]
SO₄²⁻ [36%]
OA [38%]